Applied Microbiology and Biotechnology (2018) 102:689–702
https://doi.org/10.1007/s00253-017-8648-z

BIOTECHNOLOGICAL PRODUCTS AND PROCESS ENGINEERING

Amexanthomycins A–J, pentangular polyphenols produced by *Amycolatopsis mediterranei* S699Δ*rifA*

Xiaomei Li[1] · Xingkang Wu[1] · Jing Zhu[2] · Yuemao Shen[1,2]

Received: 3 September 2017 / Revised: 8 November 2017 / Accepted: 12 November 2017 / Published online: 27 November 2017

Abstract

Ten new pentangular polyphenols, namely amexanthomycins A–J (**1**–**10**) were isolated from the strain *Amycolatopsis mediterranei* S699Δ*rifA* constructed by deleting the polyketide synthase genes responsible for the biosynthesis of rifamycins. Their structures were elucidated on the basis of 1D and 2D NMR spectroscopic data and high-resolution ESIMS. Amexanthomycins A–C (**1**–**3**) showed inhibitory activity against human DNA topoisomerases.

Keywords *Amycolatopsis mediterranei* S699 · Pentangular polyphenols · Topoisomerase IIα inhibitor · *min-PKS*

Introduction

Microorganisms, particularly actinomycetes, serve as a prolific source of structurally diverse bioactive metabolites for the pharmaceutical industry (Berdy 2005; Cragg and Newman 2013; Demain 2014). However, most of the strains belong to *Streptomyces*, with small portions from other genera called rare actinomycetes, such as *Saccharopolyspora*, *Amycolatopsis*, *Micromonospora*, *Actinoplanes*, and *Amycolatopsis* (Tiwari and Gupta 2012). Although *Amycolatopsis* is not a large group within the phylum Actinobacteria, this genus is well-known for the production of the antimicrobial agents currently available in the market such as vancomycin (glycopeptides) (Nagarajan 1991) and rifamycins (ansamycins) (August et al. 1998).

Amycolatopsis mediterranei S699 is a well-known rifamycin producer (August et al. 1998; Stratmann et al. 1999; Xu et al. 2005). Up to date, no other types of secondary metabolites were isolated from *A. mediterranei* S699. Bioinformatic analysis of the genome sequence of *A. mediterranei* S699 revealed diverse gene clusters (Verma et al. 2011). In order to exploit minor natural products with bioactivities or novel skeleton, the mutant strain *A. mediterranei* S699Δ*rifA* was constructed by deleting the polyketide synthase genes responsible for the biosynthesis of rifamycins, the main components of the wild-type strain. In this study, ten new pentangular polyphenols, namely amexanthomycins A–J (**1**–**10**), were isolated from the fermentation products of *A. mediterranei* S699Δ*rifA* on YMG agar media. Herein, we report the isolation, structure elucidation, bioactivity, and proposed biosynthetic pathway for compounds **1**–**10** (Fig. 1).

Electronic supplementary material (ESI) available: The NMR spectra and HRESIMS of all the compounds and disruption of *PKS* genes.

Electronic supplementary material The online version of this article (https://doi.org/10.1007/s00253-017-8648-z) contains supplementary material, which is available to authorized users.

✉ Yuemao Shen
yshen@sdu.edu.cn

[1] Key Laboratory of Chemical Biology (Ministry of Education), School of Pharmaceutical Sciences, Shandong University, No. 44 West Wenhua Road, Jinan, Shandong 250012, People's Republic of China

[2] State Key Laboratory of Microbial Technology, Shandong University, Jinan, Shandong 250100, People's Republic of China

Materials and methods

General experimental procedures

The NMR spectra were recorded on Bruker DRX-600 MHz NMR spectrometer (Bruker Daltonics Inc., Billerica, Massachusetts) with tetramethylsilane (TMS) as an internal standard. The HRESIMS were measured on an LTQ-Orbitrap XL. Sephadex LH-20 was obtained from GE Amersham Biosciences (Piscataway, New Jersey). Reversed-phase (RP) C_{18} silica gel for column chromatography (CC) was obtained from Merck (Darmstadt, Germany). Silica gel

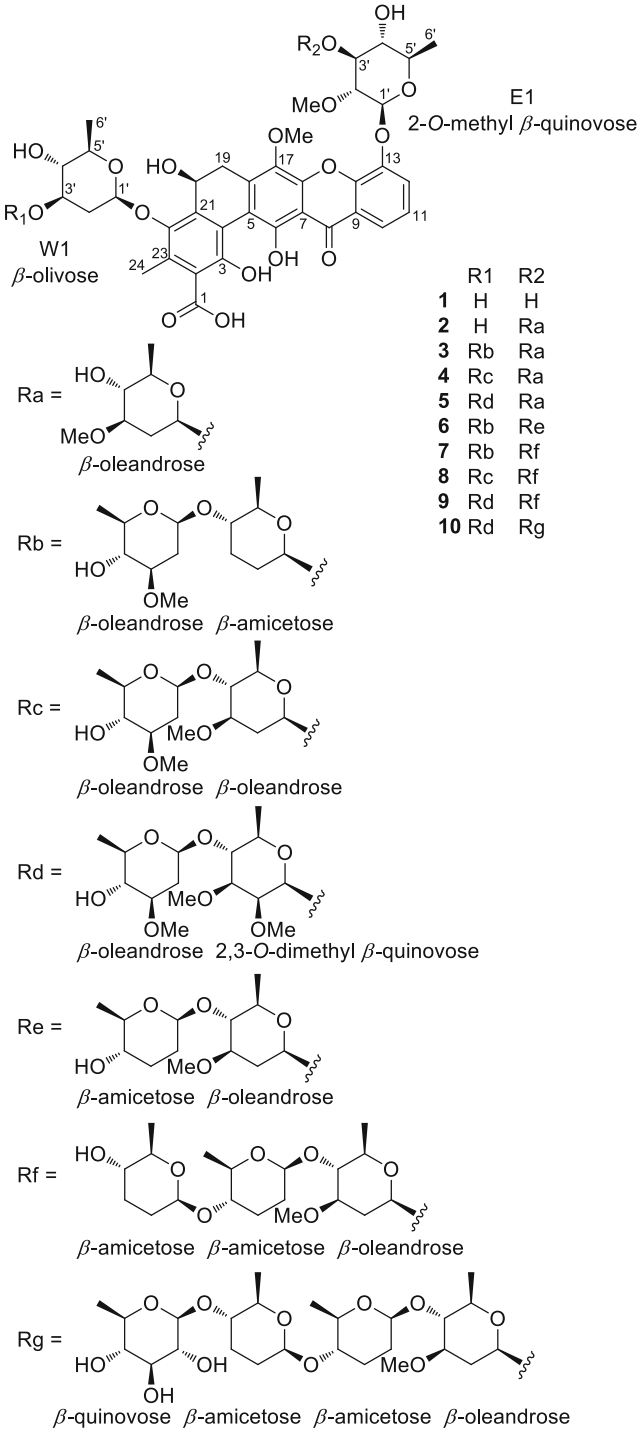

Fig. 1 Chemical structures of amexanthomycins A–J (**1**–**10**)

GF_{254} for thin-layer chromatography (TLC) was purchased from Qingdao Marine Chemical Ltd. (Qingdao, China). Semipreparative HPLC was performed on Waters 1525 Binary HPLC Pump and Waters 996 Photodiode Array Detector, equipped with an Agilent Eclipse XDB-C18 column (5 μm, 9.4 × 250 mm). Compounds were visualized under UV light and sprayed with H_2SO_4/EtOH (1:9, *v*/*v*) and vanillic aldehyde, followed by heating.

Microbial materials

Amycolatopsis mediterranei S699 strain was provided by Prof. Linquan Bai at Shanghai Jiao Tong University. It was a derivative of the original type strain (ATCC 13685) isolated in 1957 at St. Raphael, France (Kim et al. 1992; Tang et al. 2012). *A. mediterranei* S699Δ*rifA* strain was constructed by deleting the polyketide synthase genes responsible for the biosynthesis of rifamycins (Fig. S83).

Fermentation and isolation of compounds 1–10

Amycolatopsis mediterranei S699Δ*rifA* strain was cultured for 12 days on YMG (yeast extract 4 g, malt extract 10 g, glucose 4 g, ddH_2O 1000 mL, pH 7.2, agar 20 g) agar plates with a total volume of 20 L at 28 °C. The culture was diced and extracted three times overnight with EtOAc-MeOH (80:20, *v*/*v*) at room temperature to obtain the crude extract, which was partitioned between H_2O and EtOAc (1:1, *v*/*v*) until the organic layer was colorless. The EtOAc extract was partitioned between 95% aqueous MeOH and petroleum ether (PE) until the PE layer was colorless. The 95% MeOH solution was concentrated under vacuum at 37 °C to afford the defatted MeOH extract (4.1 g). The MeOH extract was subjected to column chromatography over Sephadex LH-20 eluted with MeOH to give Fr. A–E.

Fr. A (357 mg) was purified by medium pressure liquid chromatography (MPLC) over *RP-18* silica gel (30 g) eluted with gradient aqueous acetonitrile (30, 40, 50, 60, 70, 80, 90, and 100% CH_3CN, 200 mL each) to afford three fractions Fr. A1–A3. Fr. A2 (22 mg) was purified by HPLC (Agilent Eclipse XDB-C18, 5 μm, 9.4 × 250 mm; 4 mL/min; UV 274 nm) eluted with gradient acetonitrile (0 min: 45% CH_3CN; 10 min: 57% CH_3CN; 15 min: 71% CH_3CN; 16 min: 100% CH_3CN; 18 min: 100% CH_3CN; 19 min:45% CH_3CN; 21 min:45% CH_3CN) to afford **10** (t_R 9 min, 4.5 mg), **8** (t_R 12.5 min, 1.5 mg), **9** (t_R 13.3 min, 4.9 mg), and **7** (t_R 13.8 min, 4 mg) (Fig. S82).

Fr. B (1.62 g) was subjected to MPLC over *RP-18* silica gel (60 g) eluted with gradient aqueous acetonitrile (30, 50, 70, and 100% CH_3CN, 500 mL each) to afford five fractions Fr. B1–B5. Fr. B3 (475 mg) was then subjected to column chromatography over Sephadex LH-20 eluted with MeOH to afford Fr. B3a and Fr. B3b. Then they were purified by HPLC (Agilent Eclipse XDB-C18, 5 μm, 9.4 × 250 mm, 4 mL/min, UV 274 nm) eluted with gradient aqueous acetonitrile (0 min: 48% CH_3CN; 10 min: 54% CH_3CN; 15 min: 68% CH_3CN; 16 min: 100% CH_3CN; 18 min: 100% CH_3CN; 19 min: 48% CH_3CN; 21 min: 48% CH_3CN) and 43% acetonitrile to obtain **6** (t_R 11.3 min, 1.5 mg), **8** (t_R 12 min, 4.5 mg), **9** (t_R 13.2 min, 10 mg), **7** (t_R 14 min, 8.2 mg), **4** (t_R 12 min, 1.8 mg), **5** (t_R 14 min, 6.9 mg), and **3** (t_R 16 min, 4.2 mg), respectively (Fig. S82).

Fr. C (1.23 g) was subjected to MPLC over *RP-18* silica gel (60 g) eluted with gradient aqueous acetonitrile (30, 40, 50, 70, and 100% CH_3CN, 500 mL each) to afford five fractions Fr. C1–C5. Fr. C2 (100 mg) and Fr. C3 (26 mg) were purified by HPLC (Agilent Eclipse XDB-C18, 5 μm, 9.4 × 250 mm, 4 mL/min, UV 274 nm) eluted with 32 and 35% acetonitrile to afford **1** (t_R 5.7 min, 4.8 mg) and **2** (t_R 9.7 min, 4.5 mg), respectively (Fig. S82).

Results

Compound **1** was obtained as yellowish powder. Its molecular formula was determined to be $C_{37}H_{40}O_{17}$ on the basis of high-resolution ESIMS (Fig. S72) at *m/z* 757.2336 $[M + H]^+$ (calcd. for $C_{37}H_{41}O_{17}^+$, 757.2338), 779.2144 $[M + Na]^+$ (calcd. for $C_{37}H_{40}O_{17}Na^+$, 779.2158), and NMR data (Table S1, Figs. S1–5). Interpretation of the ^1H, ^{13}C, and HSQC NMR spectrum showed the presence of a ketone (δ_C 182.1), a acyl carbon (δ_C 172.3), 18 olefinic carbons, two sugar anomeric carbons (δ_C 102.2, 102.4), eight oxymethine, two methoxyl, two methylene, and three methyl groups. The ^1H-^1H COSY correlations between H-10 (δ_H 8.02)/H-11 (δ_H 7.36)/H-12 (δ_H 7.85), the HMBC correlations from H-10 to C-8 (δ_C 182.1) and C-14 (δ_C 146.5), H-11 to C-9 (δ_C 121.9) and C-13 (δ_C 146.9), and H-12 to C-10 (δ_C 118.4) and C-14 indicated the presence of the benzene ring (ring E) with substitution of oxygen at C-13 and C-14, and a ketone linked to C-9, which confirmed the presence of substructure A (Fig. 2).

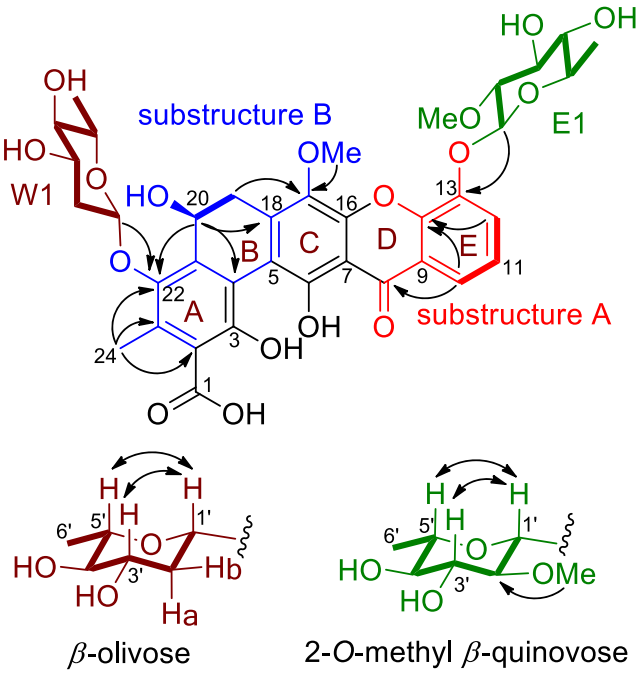

Fig. 2 Selected ^1H-^1H COSY (—), HMBC (→), and NOE (↔) correlations for **1**

The ^1H-^1H COSY correlations between H_2-19 (δ_H 2.72, 4.10) and H-20 (δ_H 5.77), along with the HMBC correlations from H_2-19 to C-5 (δ_C 115.8), C-17 (δ_C 139.1), and C-21 (δ_C 136.3); H-20 to C-4 (δ_C 118.6), C-18 (δ_C 140.7), and C-22 (δ_C 145.6); H_3-24 (δ_H 2.85) to C-2 (δ_C 126.1), C-22, and C-23 (δ_C 130.6); and 17-OMe (δ_H 4.11) to C-17 revealed the presence of substructure B including ring B (Fig. 2). The presence of rings A and C was deduced from the analysis of unsaturation degrees and the five quaternary carbons including C-1 (δ_C 172.3), C-3 (δ_C 152.8), C-6 (δ_C 152.4), C-7 (δ_C 108.5), and C-16 (δ_C 148.8). Ring C was connected to ring E via an ester bond between C-16 and C-14 and a ketone bond between C-7 and C-9, forming the ring D. The carbons C-3 and C-6 were attached to a hydroxyl group, respectively, and C-2 was attached to a carboxyl group, which was in accordance with the chemical shift and the molecular formula, and thus confirmed the aglycone moiety (Fig. 2). Furthermore, the NMR comparison with that of literature readily revealed that the aglycone moiety (rings A–E) of **1** was similar to arixanthomycin B, except for the presence of an oxazolidine ring at C-1 and C-24 and the absence of a hydroxyl group substitution at C-20 in arixanthomycin B (Kang and Brady 2014a).

The deoxysugar moiety E1 of **1** was determined by the ^1H-^1H COSY and HMBC correlations (Table S1). The ^1H-^1H COSY correlations of H-1' (δ_H 5.61)/H-2' (δ_H 3.92)/H-3' (δ_H 4.25)/H-4' (δ_H 3.87)/H-5' (δ_H 4.01)/H-6' (δ_H 1.66), and the NOE correlation between H-1' and H-5', along with the HMBC correlation from 2'-OMe (δ_H 4.18) to C-2' (δ_C 85.0) indicated the sugar moiety E1 is 2-*O*-methyl *β*-quinovose. The large constant couplings between H-1' and H-2' (7.7 Hz), H-2' and H-3' (9.0 Hz), H-3' and H-4' (9.1 Hz), and H-4' and H-5' (9.1 Hz) revealed all the protons of this deoxysugar were in the axial position, which was further confirmed by the NOE correlations between H-1' and H-3', H-1' and H-5' (Fig. 2). Similarly, the deoxysugar moiety W1 of **1** was determined to be *β*-olivose. The linkages between C-1' of E1 and C-13, and C-1' of W1 and C-22 through *O*-glycosidic bridge were revealed by the HMBC correlations from H-1' of E1 to C13, H-1' of W1 to C22, respectively. Thus, the structure of compound **1** was determined as amexanthomycin A.

Compound **2** has the molecular formula of $C_{44}H_{52}O_{20}$ based on its HRESIMS (Fig. S73) and NMR data (Table S2, Figs. S9–14). The NMR spectra of **2** were similar to that of **1**, indicating that both have the same aglycone moiety, 2-*O*-methyl *β*-quinovose (E1), and *β*-olivose (W1) moiety (Fig. 1). However, one deoxysugar moiety was demonstrated in **2** by the NMR spectra and the molecular formula (Tables 1 and 3). The long-range couplings from H-1' (δ_H 5.02) to H-6' (δ_H 1.55) and the HMBC correlations from H-6' to C-4' (δ_C 66.5), H-5' (δ_H 3.67) to C-1' (δ_H 102.3), and 3'-OMe (δ_H 3.42) to C-3' (δ_C 78.8)

Table 1 ^{1}H NMR spectroscopic data (400 MHz, C_5D_5N) for amexanthomycins A–E (**1**–**5**)

Position	δ_H (mult. *J* in Hz)				
	1	**2**	**3**	**4**	**5**
Aglycone moiety					
10	8.02 (dd, 8.0, 1.2)	8.04 (d, 7.9)	8.04 (d, 8.0)	8.04 (d, 8.0)	8.03 (d, 8.0)
11	7.36 (t, 8.0)	7.34 (t, 7.9)	7.33 (t, 8.0)	7.34 (t, 8.0)	7.36 (t, 8.0)
12	7.85 (dd, 8.0, 1.2)	7.79 (d, 7.9)	7.78 (d, 8.0)	7.79 (d, 8.0)	7.81 (d, 8.0)
19a	2.72 (dd, 16.0, 3.4)	2.73 (dd, 15.8, 3.4)	2.72 (dd, 15.9, 3.4)	2.73 (dd, 15.5, 2.8)	2.74 (dd, 15.9, 3.2)
19b	4.10 (dd, 15.9, 2.3)	4.08[a]	4.09[a]	4.11[a]	4.08[a]
20	5.77 (t, 2.9)	5.77 (t, 2.9)	5.75 (t, 3.0)	5.77 (t, 2.8)	5.78 (t, 2.8)
24	2.85 (s)	2.94 (s)	3.00 (s)	2.98 (s)	2.88 (s)
17-OMe	4.11 (s)	4.10 (s)	4.10 (s)	4.11 (s)	4.12 (s)
Sugar moieties					
W1	*β*-oli	*β*-oli	*β*-oli	*β*-oli	*β*-oli
1’	5.13 (dd, 9.8, 1.4)	5.13 (dd, 9.8, 1.4)	5.12[a]	5.14 (dd, 9.8, 1.7)	5.13 (dd, 9.7, 1.4)
2’a	2.46 (dt, 12.2, 10.2)	2.41[a]	2.24[a]	2.26[a]	2.33[a]
2’b	3.03 (ddd, 12.4, 5.0, 1.5)	3.04 (dd, 12.0, 3.7)	2.96[a]	3.03 (dd, 11.3, 4.9)	3.10 (dd, 11.4, 4.9)
3’	4.16[a]	4.19[a]	4.00[a]	4.12[a]	4.15[a]
4’	3.62[a]	3.60[a]	3.47[a]	3.52[a]	3.53[a]
5’	3.58[a]	3.55[a]	3.48[a]	3.51[a]	3.53[a]
6’	1.47 (d, 5.6)	1.45 (d, 5.7)	1.41 (d, 4.5)	1.42 (d, 4.9)	1.44 (d, 4.6)
W2			*β*-ami	*β*-ole	2,3-*O*-diMe *β*-qui
1’			4.74[a]	4.87 (dd, 9.5, 1.5)	4.80 (d, 7.8)
2’a			1.76[a]	1.78[a]	3.28 (t, 8.2)
2’b			1.97[a]	2.51[a]	
3’a			1.78[a]	3.63[a]	3.54[a]
3’b			2.48[a]		
4’			3.39[a]	3.54[a]	3.62[a]
5’			3.59[a]	3.60[a]	3.60[a]
6’			1.37 (d, 6.1)	1.40 (d, 6.0)	1.37 (d, 6.3)
2’-OMe					3.72 (s)
3’-OMe				3.53 (s)	3.79 (s)
W3			*β*-ole	*β*-ole	*β*-ole
1’			4.76 (dd, 9.8, 1.5)	4.97 (dd, 9.7, 1.5)	4.94[a]
2’a			1.73[a]	1.74[a]	1.77[a]
2’b			2.51[a]	2.56[a]	2.56[a]
3’			3.49[a]	3.50[a]	3.50[a]
4’			3.50[a]	3.51[a]	3.51[a]
5’			3.60[a]	3.62[a]	3.63[a]
6’			1.59 (d, 5.8)	1.60 (d, 6.1)	1.61 (d, 6.1)
3’-OMe			3.47 (s)	3.48 (s)	3.49 (s)
E1	2-*O*-Me *β*-qui	2-*O*-Me *β*-qui	2-*O*-Me β-qui	2-*O*-Me β-qui	2-*O*-Me β-qui
1’	5.61 (d, 7.7)	5.55 (d, 7.6)	5.55 (d, 7.7)	5.56 (d, 7.7)	5.56 (d, 7.7)
2’	3.92 (dd, 8.9, 7.9)	3.84 (dd, 8.9, 7.9)	3.84 (dd, 8.8, 8.0)	3.83 (dd, 8.9, 8.0)	3.85 (dd, 8.9, 8.0)
3’	4.25 (t, 9.0)	4.07 (t, 8.8)	4.04[a]	4.05[a]	4.05[a]
4’	3.87 (t, 9.1)	3.63[a]	3.63[a]	3.63[a]	3.65[a]
5’	4.01 (m)	3.91 (m)	3.90 (m)	3.91 (m)	3.91 (m)
6’	1.66 (d, 6.1)	1.58 (d, 6.0)	1.58 (d, 6.3)	1.59 (d, 6.3)	1.59 (d, 6.3)
2’-OMe	4.18 (s)	4.11 (s)	4.12 (s)	4.12 (s)	4.12 (s)
E2		*β*-ole	*β*-ole	*β*-ole	*β*-ole

Table 1 (continued)

Position	δ_H (mult. *J* in Hz)				
	1	**2**	**3**	**4**	**5**
1’		5.02 (dd, 8.8, 3.1)	5.02 (dd, 8.8, 3.1)	5.02 (dd, 8.8, 3.2)	5.03 (dd, 8.8, 3.1)
2’		2.42[a]	2.46[a]	2.43[a]	2.46[a]
3’		3.47[a]	3.45[a]	3.45[a]	3.47[a]
4’		3.94[a]	3.93[a]	3.94[a]	3.94[a]
5’		3.67[a]	3.67[a]	3.67[a]	3.69[a]
6’		1.55 (d, 6.2)	1.55 (d, 6.4)	1.55 (d, 6.3)	1.55 (d, 6.3)
3’-OMe		3.42 (s)	3.42 (s)	3.42 (s)	3.42 (s)

[a] Overlapped

in E2, along with the large constant couplings between H-1’ and H-2’a (8.8 Hz) and the NOE correlations between H-1’ and H-3’ (δ_H 3.47) and H-1’ and H-5’ revealed the sugar moiety E2 is a *β*-oleandrose. The deoxysugar E2 connected to E1 through *O*-glycosidic bridge between C-1’ of E2 and C-3’ (δ_C 86.6) of E1 was indicated by the HMBC correlation from H-1’ in E2 to C-3’ in E1 and the NOE correlation between H-1’ in E2 to H-3’ (δ_H 4.07) in E1. Thus, the structure of compound **2** was elucidated as amexanthomycin B.

Compound **3** was determined to have the molecular formula of $C_{57}H_{74}O_{25}$ (Fig. S74). Five anomeric carbons were observed (δ_C 102.3, 102.0, 101.9, 101.6, and 101.0) in the ^{13}C spectra, revealing the presence of five sugar residues, two more than those of compound **2** (Table 3). Analysis of the NMR spectra and the molecular formula in the same way as that of **2** showed that **2** and **3** possess the same aglycone moiety, 2-*O*-methyl *β*-quinovose (E1), *β*-oleandrose (E2), and *β*-olivose (W1) moieties, but two other deoxysugars named *β*-amicetose (W2) and *β*-oleandrose (W3) (Tables 1 and 3). The HMBC correlations from H-1’ (δ_H 4.74) in W2 to C-3’ (δ_C 80.1) in W1 and H-1’ (δ_H 4.76) in W3 to C-4’ (δ_C 80.0) in W2, along with the NOE correlations between H-1’ in W2 to H-3’ (δ_H 4.00) in W1 and H-1’ in W3 to H-4’ (δ_H 3.39) in W2 revealed that the attachment of the oligosaccharide chain in **3** was β-ole (1→4)-β-ami (1→3)-β-oli to C-22 (Table S3). Thus, the structure of compound **3** was elucidated as amexanthomycin C (Table 2).

The molecular formula of compound **4** was elucidated as $C_{58}H_{76}O_{26}$ (Fig. S75). A close NMR comparison (Tables 1 and 3) with that of **3** revealed that the only evident difference was the 3’-OMe (δ_H 3.53) in W2, indicating that the sugar moiety W2 *β*-amicetose was replaced by *β*-oleandrose, which was confirmed by the HMBC correlations from 3’-OMe to C-3’ (δ_C 79.0) in **4** (Table S4). Thus, the structure of compound **4** was elucidated as amexanthomycin D.

Compound **5** has the molecular formula of $C_{59}H_{78}O_{27}$ (Fig. S76). The NMR data (Tables 1 and 3) were closely similar to those of **4** except for the presence of the 2’-OMe (δ_H 3.72) in W2, revealing that the sugar moiety W2 *β*-oleandrose was replaced by 2,3-*O*-dimethyl *β*-quinovose, which was confirmed by the HMBC correlations from 2’-OMe to C-2’ (δ_C 84.2) in **5** (Table S5). Thus, the structure of compound **5** was elucidated as amexanthomycin E.

Compounds **6** and **7** were determined to have the molecular formula $C_{63}H_{84}O_{27}$ (Fig. S77) and $C_{69}H_{94}O_{29}$ (Fig. S78), respectively. Six anomeric carbons (δ_C 102.3, 102.2, 102.0, 101.9, 101.6, and 101.0) in **6** and seven ones (δ_C 103.5, 102.3, 102.1, 102.0, 101.9, 101.6, and 101.0) in **7** were observed in their respective ^{13}C spectrum, revealing the presence of six sugar residues in **6** and seven ones in **7**. (Tables 2 and 4) Analysis of the NMR spectrum and the molecular formula in the same way as those of **3** showed that **3**, **6**, and **7** share the same aglycone moiety, 2-*O*-methyl *β*-quinovose (E1), *β*-oleandrose (E2), *β*-olivose (W1), *β*-amicetose (W2), and *β*-oleandrose (W3) moieties, but one more deoxysugar named *β*-amicetose (E3) in **6** and two more ones in **7**. The HMBC correlations of **6** from H-1’ (δ_H 5.04) in E3 to C-4’ (δ_C 71.8) in E2 and the NOE correlation between H-1’ in E3 and H-4’ (δ_H 4.06) in E2 revealed that the attachment of the oligosaccharide chain in **6** was *β*-ami (1→4)-β-ole (1→3)-2-*O*-methyl *β*-qui to C-13 (Table S6). The HMBC correlations of **7** from H-1’ (δ_H 4.70) in E4 to C-4’ (δ_C 80.0) in E3 and the NOE correlation between H-1’ in E4 to H-4’ (δ_H 3.40) in E3 revealed that the attachment of the oligosaccharide chain in **7** was *β*-ami (1→4)-*β*-ami (1→4)-*β*-ole (1→3)-2-*O*-methyl *β*-qui to C-13 (Table S7). Thus, the structures of compounds **6** and **7** were determined as amexanthomycins F and G, respectively.

The molecular formula of compounds **8** and **9** were determined to be $C_{70}H_{96}O_{30}$ (Fig. S79) and $C_{71}H_{98}O_{31}$ (Fig. S80), respectively. Their NMR data (Tables 1 and

Table 2 ^{1}H NMR spectroscopic data (400 MHz, C_5D_5N) for amexanthomycins F–J (**6**–**10**)

Position	δ_H (mult. *J* in Hz)				
	6	**7**	**8**	**9**	**10**
Aglycone moiety					
10’	8.03 (d, 8.0)	8.02 (d, 8.0)	8.03 (d, 8.0)	8.02 (d, 8.0)	8.03 (d, 8.0)
11’	7.35 (t, 8.0)	7.34 (t, 8.0)	7.35 (t, 8.0)	7.37 (t, 8.0)	7.36 (t, 8.0)
12’	7.80 (d, 8.0)	7.81 (d, 8.0)	7.79 (d, 8.0)	7.81 (d, 8.0)	7.81 (d, 8.0)
19’a	2.73 (dd, 15.9, 3.2)	2.74 (dd, 15.8, 3.0)	2.74 (dd, 15.7, 2.9)	2.74 (dd, 15.6, 2.9)	2.74 (dd, 15.6, 2.9)
19’b	4.10[a]	4.10[a]	4.10[a]	4.13[a]	4.10[a]
20’	5.78 (t, 2.8)	5.75 (t, 2.9)	5.77 (t, 2.9)	5.77 (t, 3.0)	5.77 (t, 3.8)
24’	2.88 (s)	2.90 (s)	2.94 (s)	2.84 (s)	2.86 (s)
17’-OMe	4.12 (s)	4.12 (s)	4.10 (s)	4.12 (s)	4.12 (s)
Sugar moieties					
W1	*β*-oli	*β*-oli	*β*-oli	*β*-oli	*β*-oli
1’	5.13[a]	5.14[a]	5.14 (dd, 9.8, 1.4)	5.14 (dd, 9.7, 1.5)	5.14 (dd, 9.7, 1.5)
2’a	2.24[a]	2.25[a]	2.26[a]	2.30[a]	2.28[a]
2’b	2.96[a]	2.96 (dd, 11.3, 5.1)	3.03 (dd, 11.3, 4.6)	3.10 (dd, 11.9, 4.2)	3.10 (dd, 11.9, 4.6)
3’	4.00[a]	4.02[a]	4.11[a]	4.15[a]	4.14[a]
4’	3.48[a]	3.58[a]	3.51[a]	3.54[a]	3.51[a]
5’	3.50[a]	3.50[a]	3.52[a]	3.53[a]	3.53[a]
6’	1.44 (d, 5.1)	1.44 (d, 5.1)	1.43[a]	1.44 (d, 6.0)	1.44 (d, 6.0)
W2	*β*-ami	*β*-ami	*β*-ole	2,3-*O*-diMe *β*-qui	2,3-*O*-diMe *β*-qui
1’	4.75[a]	4.74[a]	4.87 (dd, 9.7, 1.6)	4.81 (d, 7.8)	4.80 (d, 7.7)
2’a	1.78[a]	1.78[a]	1.76[a]	3.28 (t, 8.1)	3.28 (t, 8.1)
2’b	1.99[a]	1.98[a]	2.51[a]		
3’a	2.49[a]	2.50[a]	3.61[a]	3.52[a]	3.52[a]
3’b	1.78[a]	1.79[a]			
4’	3.40[a]	3.43[a]	3.54[a]	3.60[a]	3.60[a]
5’	3.60[a]	3.60[a]	3.58[a]	3.58[a]	3.58[a]
6’	1.37 (d, 6.0)	1.37 (d, 6.1)	1.40[a]	1.37 (d, 5.6)	1.36 (d, 5.6)
2’-OMe				3.72 (s)	3.72 (s)
3’-OMe			3.53 (s)	3.79 (s)	3.79 (s)
W3	*β*-ole	*β*-ole	*β*-ole	*β*-ole	*β*-ole
1’	4.76[a]	4.77[a]	4.96[a]	4.95[a]	4.93[a]
2’a	1.74[a]	1.72[a]	1.73[a]	1.73[a]	1.73[a]
2’b	2.53[a]	2.52[a]	2.56[a]	2.56[a]	2.54[a]
3’	3.49[a]	3.50[a]	3.51[a]	3.49[a]	3.50[a]
4’	3.51[a]	3.50[a]	3.50[a]	3.51[a]	3.51[a]
5’	3.61[a]	3.61[a]	3.62[a]	3.62[a]	3.62[a]
6’	1.58 (d, 5.8)	1.59 (d, 6.0)	1.61 (d, 6.0)	1.61 (d, 6.1)	1.61 (d, 6.1)
3’-OMe	3.48 (s)	3.48 (s)	3.48 (s)	3.49 (s)	3.44 (s)
E1	2-*O*-Me *β*-qui	2-*O*-Me *β*-qui	2-*O*-Me *β*-qui	2-*O*-Me *β*-qui	2-*O*-Me *β*-qui
1’	5.56 (d, 7.5)	5.55 (d, 7.7)	5.55 (d, 7.7)	5.55 (d, 7.7)	5.55 (d, 7.7)
2’	3.84 (dd, 8.8, 8.0)	3.84 (dd, 8.8, 8.0)	3.84 (dd, 8.8, 8.0)	3.84 (dd, 8.9, 8.0)	3.81[a]
3’	4.04[a]	4.03[a]	4.03[a]	4.05 (t, 9.0)	4.01[a]
4’	3.58[a]	3.57[a]	3.57[a]	3.57[a]	3.55[a]
5’	3.94(m)	3.94(m)	3.92 (dd, 9.1, 6.2)	3.94[a]	3.92[a]
6’	1.56[a]	1.57[a]	1.56 (d, 5.8)	1.56[a]	1.55 (d, 6.3)
2-OMe	4.12 (s)	4.13 (s)	4.12 (s)	4.13 (s)	4.13 (s)
E2	β-ole	β-ole	β-ole	β-ole	*β*-ole

Table 2 (continued)

Position	δ_H (mult. *J* in Hz)				
	6	**7**	**8**	**9**	**10**
1’	5.00 (dd, 9.8, 1.9)	4.99[a]	4.99[a]	5.00[a]	4.98 (dd, 9.6, 1.6)
2’a	2.33[a]	2.31[a]	2.31[a]	2.32[a]	2.20[a]
2’b	2.46[a]	2.46[a]	2.46[a]	2.45[a]	2.45 (dd, 9.3, 3.2)
3’	3.46[a]	3.45[a]	3.46[a]	3.45[a]	3.45[a]
4’	4.06[a]	4.02[a]	4.02[a]	4.04[a]	4.00[a]
5’	3.68[a]	3.67[a]	3.68[a]	3.67[a]	3.66[a]
6’	1.54[a]	1.54[a]	1.54 (d, 5.8)	1.54[a]	1.54[a]
3-OMe	3.45 (s)	3.42 (s)	3.41 (s)	3.41 (s)	3.40 (s)
E3	*β*-ami	*β*-ami	*β*-ami	*β*-ami	*β*-ami
1’	5.04 (dd, 9.0, 1.4)	4.96[a]	4.95[a]	4.98[a]	4.94[a]
2’a	1.80[a]	1.76[a]	1.76[a]	1.75[a]	1.76[a]
2’b	2.14[a]	2.10[a]	2.08[a]	2.10[a]	2.08[a]
3’a	2.16[a]	1.76[a]	1.75[a]	1.75[a]	1.73[a]
3’b	2.20[a]	2.45[a]	2.45[a]	2.44[a]	2.41[a]
4’	3.55[a]	3.40[a]	3.39[a]	3.39[a]	3.31[a]
5’	3.59[a]	3.51[a]	3.53[a]	3.54[a]	3.50[a]
6’	1.59 (d, 6.0)	1.43 (d, 6.0)	1.42 (d, 6.0)	1.43 (d, 6.0)	1.39 (d, 6.1)
E4		*β*-ami	*β*-ami	*β*-ami	*β*-ami
1’		4.70[a]	4.70 (dd, 8.8, 1.9)	4.70 (dd, 8.8, 1.9)	4.63 (dd, 9.4, 2.2)
2’a		1.95[a]	1.94[a]	1.94[a]	1.91[a]
2’b		1.75[a]	1.75[a]	1.76[a]	1.73[a]
3’a		2.20[a]	2.20[a]	2.20[a]	2.51[a]
3’b		1.75[a]	1.74[a]	1.75[a]	1.75[a]
4’		3.50[a]	3.50[a]	3.50[a]	3.51[a]
5’		3.59[a]	3.60[a]	3.59[a]	3.61[a]
6’		1.56[a]	1.55 (d, 6.0)	1.55 (d, 6.0)	1.63 (d, 6.1)
E5					*β*-qui
1’					4.76 (d, 7.7)
2’					4.36 (dd, 9.1, 7.8)
3’					4.09[a]
4’					4.06[a]
5’					3.82[a]
6’					1.56 (d, 6.3)

[a] Overlapped

4) were closely similar to those of **7**, except that the 3’-OMe (δ_H 3.53) in W2 in **8** and 2’-OMe (δ_H 3.72) and 3’-OMe (δ_H 3.79) in W2 in **9** were present, revealing that the sugar moiety W2 *β*-amicetose was replaced by *β*-oleandrose in **8** and 2,3-*O*-dimethyl *β*-quinovose in **9**, which was confirmed by the HMBC correlations from 3’-OMe to C-3’ (δ_C 79.1) in W2 in **8**, from 2’-OMe to C-2’ (δ_C 84.2), and from 3’-OMe to C-3 (δ_C 84.9) in W2 in **9** (Tables S8 and S9). Thus, the structures of compounds **8** and **9** were determined as amexanthomycins H and I, respectively.

Compound **10** was elucidated as $C_{77}H_{108}O_{35}$ (Fig. S81). Eight anomeric carbons were observed (δ_C 106.6, 103.3, 102.3, 102.1, 101.9, 101.8, 101.7, and 100.6) in the ^{13}C spectrum, revealing the presence of eight sugar residues, one more than those of compound **9** (Table 4). Analysis of the NMR spectrum and the molecular formula in the same way as that of **7** showed that **9** and **10** possess the same aglycone moiety, 2-*O*-methyl *β*-quinovose (E1), *β*-oleandrose (E2), *β*-amicetose (E3), *β*-amicetose (E4), *β*-olivose (W1), 2,3-*O*-dimethyl *β*-quinovose (W2), and *β*-oleandrose (W3) moieties, but one more deoxysugar

Table 3 ^{13}C NMR spectroscopic data (151 MHz, C_5D_5N) for amexanthomycins A–E (**1**–**5**)

Aglycone moiety	**1**	**2**	**3**	**4**	**5**	Sugar moieties	**1**	**2**	**3**	**4**	**5**
1	172.3s	172.1s	172.2s	172.2s	172.4s	W1	*β*-oli	*β*-oli	*β*-oli	*β*-oli	*β*-oli
2	126.1s	124.2s	123.8s	124.0s	125.0s	1’	102.4d	102.4d	102.0d	102.0d	101.8d
3	152.8s	153.7s	157.1s	nd	153.7s	2’	40.5t	40.5t	37.8t	37.6t	37.5t
4	118.6s	119.2s	119.5s	119.3s	118.9s	3’	71.6d	71.6d	80.1d	79.7d	80.1d
5	115.8s	116.7s	117.0s	116.9s	116.2s	4’	77.8d	77.8d	75.2d	75.0d	75.0d
6	152.4	nd	154.0s	nd	153.3s	5’	73.9d	73.8d	73.3d	73.3d	73.3d
7	108.5s	109.5s	109.8s	109.7s	109.0s	6’	17.9q	17.9q	17.8q	17.9q	17.9q
8	182.1s	181.2s	180.9s	nd	181.7s	W2			*β*-ami	*β*-ole	2,3-*O*-diMe *β*-qui
9	121.9s	122.5s	122.7s	122.6s	122.2s	1’			101.0d	98.6d	101.9d
10	118.4d	118.8d	118.8d	118.8d	118.7d	2’			31.3t	37.4t	84.2d
11	124.5d	124.2d	124.1d	124.2d	124.4d	3’			30.7t	79.0d	84.9d
12	121.0d	120.6d	120.6d	120.4d	120.6d	4’			80.0d	82.5d	82.3d
13	146.9s	146.6s	146.6s	146.6s	146.6s	5’			75.1d	71.9d	71.5d
14	146.5s	146.3s	146.2s	146.2s	146.3s	6’			18.3q	18.5d	18.2d
16	148.8s	149.1s	149.5s	149.5s	149.0s	2’-OMe					60.61q
17	139.1s	138.9s	138.8s	138.8s	139.0s	3’-OMe				57.4q	60.6q
18	140.7s	140.4s	140.1s	140.2s	140.6s	W3			β-ole	β-ole	β-ole
19	30.8t	30.7t	30.7t	30.7t	30.8t	1’			101.6d	100.3d	100.6d
20	60.7d	60.7d	60.8d	60.7 d	60.8d	2’			37.2t	37.3t	37.4t
21	136.3s	136.7s	136.8s	136.1s	136.5s	3’			81.5d	81.6d	81.6d
22	145.6s	145.2s	144.8s	144.9s	145.1s	4’			76.3d	76.3d	76.3d
23	130.6s	131.7s	132.1s	131.2s	131.2s	5’			72.9d	73.0d	73.1d
24	14.9q	15.3q	15.5q	15.5q	15.2q	6’			18.8d	18.8q	18.7q
17-OMe	61.7q	61.8q	61.7q	61.8q	61.8q	3-OMe			57.1q	57.1q	57.1q
						E1	2-*O*-Me *β*-qui	2-*O*-Me *β*-qui	2-*O*-Me *β*-qui	2-*O*-Me *β*-qui	2-*O*-Me *β*-qui
						1’	102.2d	101.9d	101.9d	101.9d	101.9d
						2’	85.0d	83.3d	83.3d	83.3d	83.3d
						3’	77.1d	86.6d	86.6d	86.6d	86.6d
						4’	76.4d	74.4d	74.4d	74.4d	74.4d
						5’	73.4d	72.9d	72.9d	72.9d	72.9d
						6’	18.6q	18.3q	18.4q	18.3q	18.3q
						2-OMe	61.4q	61.6q	61.6q	61.6q	61.6q
						E2		*β*-ole	*β*-ole	*β*-ole	*β*-ole
						1’		102.3d	102.3d	102.3d	102.3d
						2’		32.7t	32.7t	32.7t	32.7t
						3’		78.8d	78.8d	78.8d	78.8d
						4’		66.5d	66.5d	66.5d	66.5d
						5’		72.0d	72.0d	72.0d	72.0d
						6’		17.3q	17.3q	17.3q	17.3q
						3’-OMe		55.5q	55.5q	55.5q	55.5q

nd not observed and defined

named *β*-quinovose (E5) in **10** than in **9** (Tables 2 and 4). The HMBC correlations from H-1’ (δ_H 4.76) in E5 to C-4’ (δ_C 80.7) in E4 and the NOE correlation between H-1’ in E5 to H-4’ (δ_H 3.51) in E4 revealed that the attachment of the oligosaccharide chain in **10** was *β*-qui (1→4)-*β*-ami (1→4)-*β*-ami (1→4)-*β*-ole (1→3)-2-*O*-methyl *β*-qui to C-13 (Table S10). Thus, the structure of compound **10** was determined as amexanthomycin J.

The structures of amexanthomycins A–J (**1**–**10**) feature a xanthone-containing pentangular polyphenol core. The xanthone derivatives have been reported to function as DNA topoisomerase II inhibitors (Woo et al. 2007; Woo et al. 2010). Thus, we assessed the topoisomerases IIα (Topo IIα) inhibitory activities of **1**–**10** using Topo-mediated supercoiled DNA relaxation assay (Zhang et al. 2017). Compounds **1**–**3** exhibited Topo IIα inhibitory activity at 500 μM, while **4**–**10** showed no activities (Fig. 3a). The dose-dependent assays showed that **1** and **2** had stronger Topo IIα inhibitory activity than **3** (Fig. 3b). These results indicated that the number and type of deoxysugar substitutions in amexanthomycins had impact on the topoisomerase inhibitory activities, which provided valuable information regarding structure–activity relationships for the development of new topoisomerase inhibitors.

Discussion

It has been more than half a century since rifamycins were isolated from *Amycolatopsis mediterranei* S699 (Sensi et al. 1959). The semisynthetic derivatives of rifamycin B have been used against *Mycobacterium tuberculosis* (Woodley and Kilburn 1982). Thus, *A. mediterranei* S699 has been the focus for researchers to explore the biosynthesis of rifamycins, making it one of the most thoroughly studied strains (August et al. 1998; Tang et al. 2012; Verma et al. 2011; Xu et al. 2005; Yu et al. 2001). However, as of today, no other types of secondary metabolites isolated from *A. mediterranei* S699 were reported. In our continuing studies on *A. mediterranei* S699, ten new pentangular polyphenols, namely amexanthomycins A–J (**1**–**10**) were obtained from the mutant strain S699Δ*rifA* constructed by deleting the polyketide synthase genes responsible for the biosynthesis of rifamycins (Fig. S83). It is possible that the production of amexanthomycins was inhibited by the main products rifamycins in the wild strain S699; nevertheless, the gene cluster of amexanthomycins was activated after inactivation of rifamycins in the mutant strain S699Δ*rifA*. Another possibility is that the minor components of amexanthomycins were difficult to be detected with the background of rifamycins in S699, while in S699Δ*rifA*, amexanthomycins turned to be the main products and were easier to be detected without the influence of rifamycins. It is most possible that S699Δ*rifA* was cultured on agar plates, while S699 was usually studied in shake flask culture (Ma et al. 2008; Xu et al. 2003), and the change of cultivation condition led to the production of amexanthomycins. It needs to be further studied how amexanthomycins were activated or detected in S699Δ*rifA*.

The amexanthomycins shared the similar aglycone moiety of xanthone-containing pentangular polyphenol with arixanthomycin A (Kang and Brady 2014a) or calixanthomycin A (Kang and Brady 2014b), except for the absence of an oxazolidine or lactone ring at C-1 and C-24. And the substituted positions of hydroxyl or methoxyl group in amexanthomycins were different from the two reported compounds. Furthermore, the oligosaccharide chains were linked to C-13 and C-22, respectively, and there were eight deoxysugar substitutions in amexanthomycin J, which were first reported in this literature.

In silico genome analyses with the antibiotics and Secondary Metabolite Analysis Shell (antiSMASH) algorithm revealed that the gene cluster of *GC22* in *Amycolatopsis mediterranei* S699 was involved in the biosynthesis of amexanthomycins (Table S13) (Verma et al. 2011), which was further confirmed by the deletion of the minimal polyketide synthase (*min-PKS*) of *GC22* to obtain the mutant strain S699Δ*rifA*Δ*PKS* without the production of amexanthomycins (Fig. 4). Thus, the gene cluster responsible for amexanthomycins was identified, which provides strong support for exploring the biosynthesis of amexanthomycins. The min-PKS consists of two ketosynthase units (KS_α and KS_β, or chain length factor (CLF)) and an acyl carrier protein (ACP), which catalyzes the iterative condensation of malonyl-CoA into polyketide chains ranging from 16 to 30 carbons to form structurally diverse aromatic polyketides of secondary metabolites (Hertweck 2009; Hertweck et al. 2007). Accordingly, we proposed the biosynthetic pathway of amexanthomycins (Fig. 5). The pentacyclic xanthone core was predicted to be generated by min-PKS synthase, cyclase, and oxidoreductase using an acetyl-CoA starter unit and 11 malonyl-CoA extender units, which was followed by an oxidative rearrangement catalyzed by the predicted Bayer-Villiger oxidase (BVO). Finally, this aglycone was glycosylated by the glycosyl transferases, completing the biosynthesis of compounds **1**–**10**.

Funding information This work was supported by the National Natural Science Foundation of China (81373304, 81673317), Science Foundation of Two Sides of Strait (U1405223), and Program for Changjiang Scholars and Innovative Research Team in University (IRT_17R68).

Compliance with ethical standards This article does not contain any studies with human participants or animals performed by any of the authors.

Conflict of interest The authors declare that they have no conflict of interest.

Table 4 ^{13}C NMR spectroscopic data (151 MHz, C_5D_5N) for amexanthomycins F–J (**6**–**10**)

Aglycone moiety	**6**	**7**	**8**	**9**	**10**	Sugar moieties	**6**	**7**	**8**	**9**	**10**
1	172.4s	172.4s	172.3s	172.4s	172.4s	W1	*β*-oli	*β*-oli	*β*-oli	*β*-oli	*β*-oli
2	125.2s	125.7s	125.0s	125.9s	125.5s	1’	102.0d	102.0d	102.0d	101.8d	101.8d
3	154.0s	153.0s	153.9s	153.0s	153.3s	2’	37.8t	37.8t	37.7t	37.5t	37.5t
4	118.9s	118.8s	119.1s	118.7s	118.8s	3’	80.1d	80.1d	79.8d	80.1d	79.9d
5	116.2s	116.0s	116.4s	115.9s	116.0s	4’	75.2d	75.0d	75.1d	75.0d	74.9d
6	153.2s	151.3s	153.4s	152.8s	153.1s	5’	73.4d	73.4d	73.4d	73.3d	73.3d
7	108.9s	108.7s	109.1s	109.0s	108.7s	6’	17.9q	17.9q	17.9q	17.9q	17.9q
8	181.7s	181.9s	181.5s	182.0s	181.8s	W2	*β*-ami	*β*-ami	*β*-ole	2,3-*O*-diMe *β*-qui	2,3-*O*-diMe *β*-qui
9	122.2s	122.0s	122.3s	121.9s	120.0s	1’	101.0d	101.0d	98.7d	101.9d	101.8d
10	118.7d	118.6d	118.7d	118.6d	118.6d	2’	31.3t	31.3t	37.4t	84.2d	84.1d
11	124.4d	124.4d	124.3d	124.5d	124.4d	3’	30.7t	30.7t	79.1d	84.9d	84.8d
12	120.9d	121.0d	120.8d	121.0d	120.8d	4’	80.0d	80.1d	82.5d	82.3d	82.3d
13	146.6s	146.6s	146.6s	146.6s	146.6s	5’	75.1d	75.2d	71.9d	71.5d	71.5d
14	146.3s	146.4s	146.3s	146.4s	146.3s	6’	18.3q	18.3q	18.5q	18.2d	18.2d
16	148.9s	148.9s	149.0s	148.8s	148.9s	2’-OMe				60.63q	60.64q
17	139.0s	139.1s	139.0s	139.1s	139.0s	3’-OMe			57.4q	60.61q	60.61q
18	140.6s	140.7s	140.5s	140.7s	140.6s	W3	*β*-ole	*β*-ole	*β*-ole	*β*-ole	*β*-ole
19	30.8t	30.8t	30.8t	30.8t	30.8t	1’	101.6d	101.6d	100.3d	100.6d	100.6d
20	60.7d	60.7d	60.7d	60.7d	60.7d	2’	37.2t	37.2t	37.3t	37.4t	37.4t
21	136.4s	136.3s	136.5s	136.3s	136.4s	3’	81.5d	81.5d	81.6d	81.6d	81.5d
22	145.2s	145.4s	145.2s	145.3s	145.2s	4’	76.3d	76.3d	76.3d	76.3d	76.2d
23	131.1s	130.8s	130.3s	130.8s	131.0s	5’	72.9d	72.9d	73.0d	73.1d	73.1d
24	15.2q	15.1q	15.2q	15.0q	15.1q	6’	18.8d	18.8d	18.8d	18.7q	18.7q
17-OMe	61.8q	61.8q	61.7q	61.8q	61.8q	3-OMe	57.1q	57.1q	57.1q	57.1q	57.1q
						E1	2-*O*-Me *β*-qui	2-*O*-Me *β*-qui	2-*O*-Me *β*-qui	2-*O*-Me *β*-qui	2-*O*-Me *β*-qui
						1’	101.9d	101.9d	101.9d	102.0d	101.9d
						2’	83.3d	83.3d	83.3d	83.3d	83.3d
						3’	86.6d	86.9d	86.8d	86.6d	86.8d
						4’	74.3d	74.3d	74.3d	74.3d	74.3d
						5’	72.8d	72.8d	72.8d	72.8d	72.8d
						6’	18.4q	18.4q	18.3q	18.2q	17.5q
						2-OMe	61.6q	61.6q	61.6q	61.6q	61.6q
						E2	*β*-ole	*β*-ole	*β*-ole	*β*-ole	*β*-ole
						1’	102.2d	102.3d	102.3d	102.3d	102.3d
						2’	32.7t	32.7t	32.7t	32.7t	32.7t
						3’	79.6d	79.5d	79.5d	79.5d	79.5d
						4’	71.8d	71.8d	71.8d	71.8d	71.8d
						5’	71.5d	71.4d	71.4d	71.4d	71.4d
						6’	17.6q	17.6q	17.6q	17.6q	17.6q
						3-OMe	55.3q	56.3q	56.3q	56.3q	56.3q
						E3	*β*-ami	*β*-ami	*β*-ami	*β*-ami	*β*-ami
						1’	102.3d	102.1d	102.1d	102.1d	102.1d
						2’	31.8t	31.4t	31.4t	31.4t	31.4t
						3’	32.3t	30.9t	30.9t	30.9t	30.9t
						4’	71.4d	80.0d	80.1d	80.1d	80.1d
						5’	77.0d	75.1d	75.0d	75.0d	75.0d

Table 4 (continued)

Aglycone moiety	6	7	8	9	10	Sugar moieties	6	7	8	9	10
						6’	19.0q	18.6q	18.6q	18.6q	18.6q
						E4		*β*-ami	*β*-ami	*β*-ami	*β*-ami
						1’		103.5d	103.5d	103.5d	103.3d
						2’		31.9t	31.9t	31.9t	31.6t
						3’		32.3t	32.3t	32.3t	31.1t
						4’		71.3d	71.3d	71.3d	80.7d
						5’		76.9d	76.9d	76.9d	75.2d
						6’		19.0q	19.0q	19.0q	18.9q
						E5					*β*-qui
						1’					106.7d
						2’					72.3d
						3’					75.3d
						4’					72.7d
						5’					71.3d
						6’					18.7q

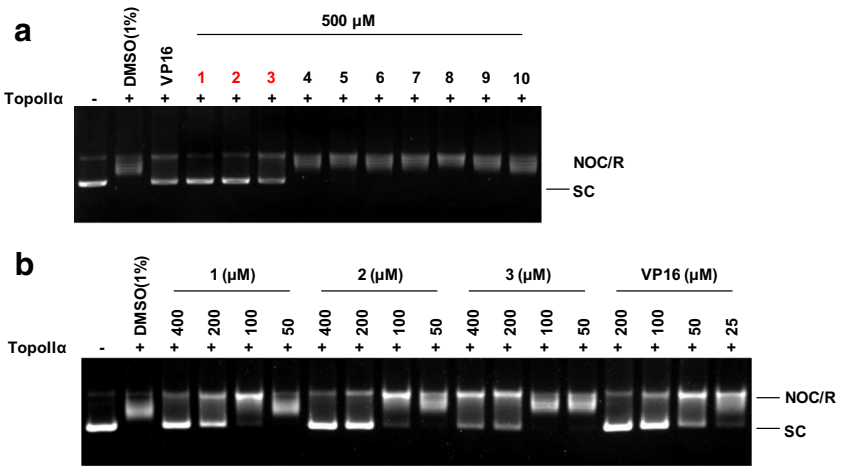

Fig. 3 Topoisomerase IIα inhibitory activities of amexanthomycins A–J (**1**–**10**) isolated from *Amycolatopsis mediterranei* S699 ΔrifA. **a** The effects of amexanthomycins A–J (**1**–**10**) on the DNA relaxation activity by Topo IIα. Supercoiled pBR322 DNA (SC) was relaxed by Topo IIα alone or with 500 μM of compounds **1**–**10**. Relaxation reaction products containing nicked open circular or relaxed DNA (NOC/R) were indicated. Etoposide (VP16) was known inhibitors of topoisomerase II and used as positive controls. **b** Compounds **1**–**3** inhibited Topo IIα mediated DNA relaxation in a dose-dependent manner

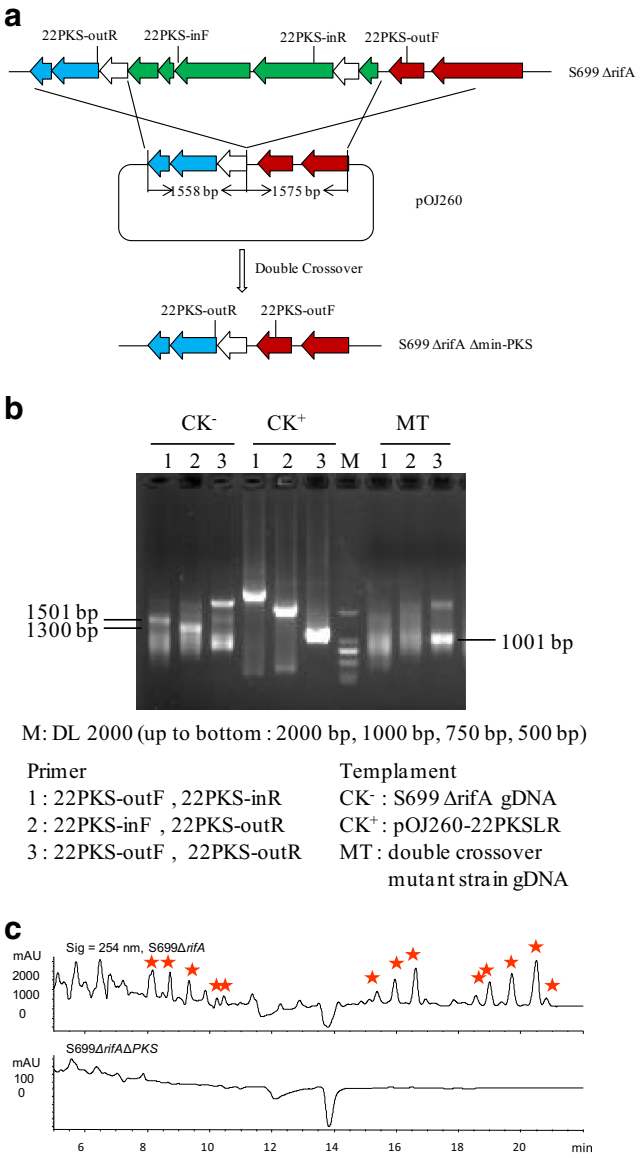

Fig. 4 Disruption of *PKS* genes. **a** Scheme of the gene inactivation of *PKS* genes. **b** PCR amplification using check primers confirmed the genotype of double crossover mutants. **c** Comparison of the HPLC profiles between the extracts of *Amycolatopsis mediterranei* S699Δ*rifA* and *Amycolatopsis mediterranei* S699Δ*rifA*Δ*PKS*

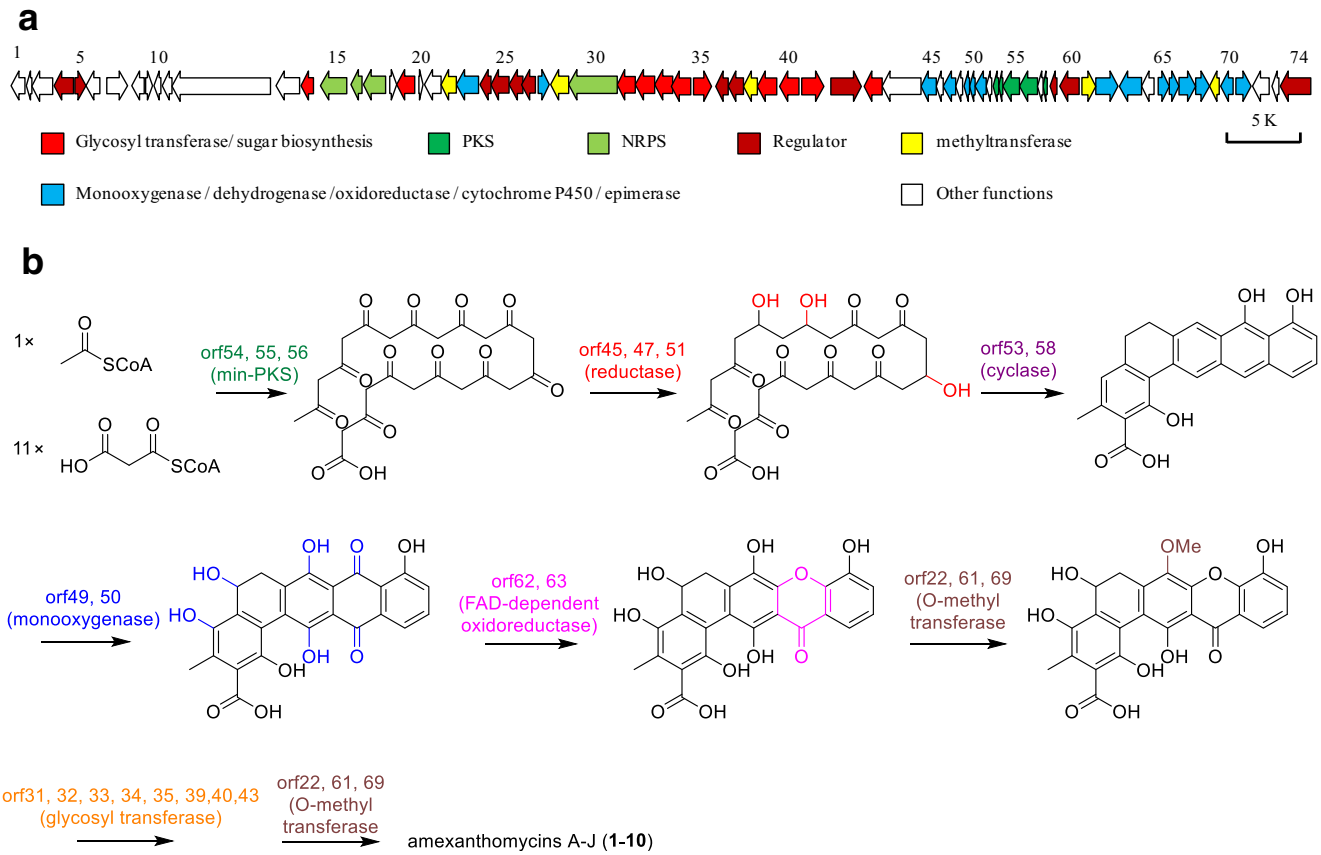

Fig. 5 **a** Amexanthomycin gene cluster (MIBiG BGC-ID: BGC0000200_c1). **b** Proposed biosynthetic pathway for amexanthomycins

References

August PR, Tang L, Yoon YJ, Ning S, Muller R, Yu TW, Taylor M, Hoffmann D, Kim CG, Zhang X, Hutchinson CR, Floss HG (1998) Biosynthesis of the ansamycin antibiotic rifamycin: deductions from the molecular analysis of the *rif* biosynthetic gene cluster of *Amycolatopsis mediterranei* S699. Chem Biol 5(2):69–79. https://doi.org/10.1016/S1074-5521(98)90141-7

Berdy J (2005) Bioactive microbial metabolites. J Antibiot (Tokyo) 58(1): 1–26. https://doi.org/10.1038/ja.2005.1

Cragg GM, Newman DJ (2013) Natural products: a continuing source of novel drug leads. Biochim Biophys Acta 1830(6):3670–3695. https://doi.org/10.1016/j.bbagen.2013.02.008

Demain AL (2014) Importance of microbial natural products and the need to revitalize their discovery. J Ind Microbiol Biotechnol 41(2):185–201. https://doi.org/10.1007/s10295-013-1325-z

Hertweck C (2009) The biosynthetic logic of polyketide diversity. Angew Chem Int Ed Engl 48(26):4688–4716. https://doi.org/10.1002/anie.200806121

Hertweck C, Luzhetskyy A, Rebets Y, Bechthold A (2007) Type II polyketide synthases: gaining a deeper insight into enzymatic teamwork. Nat Prod Rep 24(1):162–190. https://doi.org/10.1039/b507395m

Kang HS, Brady SF (2014a) Arixanthomycins A-C: phylogeny-guided discovery of biologically active eDNA-derived pentangular polyphenols. ACS Chem Biol 9(6):1267–1272. https://doi.org/10.1021/cb500141b

Kang HS, Brady SF (2014b) Mining soil metagenomes to better understand the evolution of natural product structural diversity: pentangular polyphenols as a case study. J Am Chem Soc 136(52): 18111–18119. https://doi.org/10.1021/ja510606j

Kim CG, Kirschning A, Bergon P, Ahn Y, Wang JJ, Shibuya M, Floss HG (1992) Formation of 3-amino-5-hydroxybenzoic acid, the precursor of Mc(7)N units in ansamycin antibiotics, by a new variant of the shikimate pathway. J Am Chem Soc 114:4941-4943 doi: Doi https://doi.org/10.1021/Ja00038a090

Ma FX, Kim JH, Kim SB, Seo YG, Chang YK, Hong SK, Kim CJ (2008) Medium optimization for enhanced production of rifamycin B by *Amycolatopsis mediterranei* S699: combining a full factorial design and a statistical approach. Process Biochem 43(9):954–960. https://doi.org/10.1016/j.procbio.2008.04.021

Nagarajan R (1991) Antibacterial activities and modes of action of vancomycin and related glycopeptides. Antimicrob Agents Chemother 35(4):605–609. https://doi.org/10.1128/AAC.35.4.605

Sensi P, Margalith P, Timbal MT (1959) Rifomycin, a new antibiotic; preliminary report. Farmaco Sci 14(2):146–147

Stratmann A, Toupet C, Schilling W, Traber R, Oberer L, Schupp T (1999) Intermediates of rifamycin polyketide synthase produced by an *Amycolatopsis mediterranei* mutant with inactivated *rifF* gene. Microbiology 145(12):3365–3375. https://doi.org/10.1099/00221287-145-12-3365

Tang B, Zhao W, Zheng H, Zhuo Y, Zhang L, Zhao GP (2012) Complete genome sequence of *Amycolatopsis mediterranei* S699 based on de novo assembly via a combinatorial sequencing strategy. J Bacteriol 194(20):5699–5700. https://doi.org/10.1128/JB.01295-12

Tiwari K, Gupta RK (2012) Rare actinomycetes: a potential storehouse for novel antibiotics. Crit Rev Biotechnol 32(2):108–132. https://doi.org/10.3109/07388551.2011.562482

Verma M, Kaur J, Kumar M, Kumari K, Saxena A, Anand S, Nigam A, Ravi V, Raghuvanshi S, Khurana P, Tyagi AK, Khurana JP, Lal R (2011) Whole genome sequence of the rifamycin B-producing strain

Amycolatopsis mediterranei S699. J Bacteriol 193(19):5562–5563. https://doi.org/10.1128/JB.05819-11

Woo S, Jung J, Lee C, Kwon Y, Na Y (2007) Synthesis of new xanthone analogues and their biological activity test—cytotoxicity, topoisomerase II inhibition, and DNA cross-linking study. Bioorg Med Chem Lett 17(5):1163–1166. https://doi.org/10.1016/j.bmcl.2006.12.030

Woo S, Kang DH, Nam JM, Lee CS, Ha EM, Lee ES, Kwon Y, Na Y (2010) Synthesis and pharmacological evaluation of new methyloxiranylmethoxyxanthone analogues. Eur J Med Chem 45(9):4221–4228. https://doi.org/10.1016/j.ejmech.2010.06.017

Woodley CL, Kilburn JO (1982) In vitro susceptibility of Mycobacterium avium complex and Mycobacterium tuberculosis strains to a spiropiperidyl rifamycin. Am Rev Respir Dis 126(3):586–587. https://doi.org/10.1164/arrd.1982.126.3.586

Xu J, Mahmud T, Floss HG (2003) Isolation and characterization of 27-*O*-demethylrifamycin SV methyltransferase provides new insights into the post-PKS modification steps during the biosynthesis of the antitubercular drug rifamycin B by *Amycolatopsis mediterranei* S699. Arch Biochem Biophys 411(2):277–288. https://doi.org/10.1016/S0003-9861(03)00004-3

Xu J, Wan E, Kim CJ, Floss HG, Mahmud T (2005) Identification of tailoring genes involved in the modification of the polyketide backbone of rifamycin B by *Amycolatopsis mediterranei* S699. Microbiology 151(8):2515–2528. https://doi.org/10.1099/mic.0.28138-0

Yu TW, Muller R, Muller M, Zhang X, Draeger G, Kim CG, Leistner E, Floss HG (2001) Mutational analysis and reconstituted expression of the biosynthetic genes involved in the formation of 3-amino-5-hydroxybenzoic acid, the starter unit of rifamycin biosynthesis in *Amycolatopsis Mediterranei* S699. J Biol Chem 276(16):12546–12555. https://doi.org/10.1074/jbc.M009667200

Zhang ZQ, Wu XK, Song RT, Zhang JL, Wang HX, Zhu J, Lu CH, Shen YM (2017) Ansavaricins F-I, new DNA topoisomerase inhibitors produced by *Streptomyces* sp S012. RSC Adv 7(24):14857–14867. https://doi.org/10.1039/c7ra00961e